Dynamics and segregation of cell–matrix adhesions in cultured fibroblasts

Eli Zamir*, Menachem Katz*, Yehudit Posen*, Noam Erez*, Kenneth M. Yamada†, Ben-Zion Katz‡, Shin Lin§, Diane C. Lin§, Alexander Bershadsky*, Zvi Kam* and Benjamin Geiger*¶

**Department of Molecular Cell Biology, The Weizmann Institute of Science, Rehovot 76100, Israel*
†Craniofacial Development Biology and Regeneration Branch, NIDCR, NIH, Bethesda, Maryland 20892-4370, USA
‡The Hematology Institute, Tel-Aviv Medical Center, Tel-Aviv 64239, Israel
§Department of Developmental and Cell Biology, University of California at Irvine, Irvine, California 92697-7450, USA
¶e-mail: Benny.Geiger@weizmann.ac.il

Here we use time-lapse microscopy to analyse cell–matrix adhesions in cells expressing one of two different cytoskeletal proteins, paxillin or tensin, tagged with green fluorescent protein (GFP). Use of GFP–paxillin to analyse focal contacts and GFP–tensin to study fibrillar adhesions reveals that both types of major adhesion are highly dynamic. Small focal contacts often translocate, by extending centripetally and contracting peripherally, at a mean rate of 19 micrometres per hour. Fibrillar adhesions arise from the medial ends of stationary focal contacts, contain $\alpha_5\beta_1$ integrin and tensin but not other focal-contact components, and associate with fibronectin fibrils. Fibrillar adhesions translocate centripetally at a mean rate of 18 micrometres per hour in an actomyosin-dependent manner. We propose a dynamic model for the regulation of cell–matrix adhesions and for transitions between focal contacts and fibrillar adhesions, with the ability of the matrix to deform functioning as a mechanical switch.

Cell adhesion plays a critical part in embryonic development and in regulating tissue architecture, tissue function, and signalling across cell membranes[1–5]. Adhesion complexes show extraordinary structural and molecular diversity[3,6,7]. For example, sites of cell adhesion to the extracellular matrix (ECM) can be mediated by a variety of matrix molecules and integrin proteins[8,9]. Integrins act as transmembrane linkers between ECM molecules and cytoplasmic proteins that anchor the actin cytoskeleton to the membrane.

We have shown previously that ECM adhesions formed by cultured fibroblasts can be classified by molecular and structural criteria into two major types, characterized by distinct complements of integrins and cytoskeletal anchor molecules[10,11]. Classical 'focal contacts' are located mainly at the cell periphery and contain relatively high levels of vinculin, paxillin and proteins with phosphorylated tyrosine residues, as well as integrin $\alpha_v\beta_3$. In contrast, 'fibrillar adhesions' are characteristically elongated or beaded structures, are located more centrally in cells, are enriched in tensin and $\alpha_5\beta_1$ integrin, and are associated with fibronectin fibrils[10,11]. The formation of fibrillar adhesions is affected by the rigidity or deformability of the ECM. Thus, covalent immobilization of substrate-associated fibronectin (an ECM component) blocks the formation of fibrillar adhesions and instead induces formation of large focal contacts containing both $\alpha_5\beta_1$ and $\alpha_v\beta_3$ integrin, as well as relatively high levels of tensin, vinculin, paxillin and phosphotyrosine residues[11]. We propose that the formation of fibrillar adhesions depends on ECM reorganization and a corresponding segregation of associated cellular components from focal contacts.

Here we searched for dynamic processes that might be responsible for molecular diversification of cell–matrix adhesions. We used quantitative immunofluorescence and time-lapse fluorescence microscopy to follow the reorganization of tensin and paxillin in cells transfected with GFP chimaeras of these proteins. We describe extensive modulations of focal-contact structure and localization, and show directly that fibrillar adhesions are assembled at the medial margins of classical focal contacts and transported in an actomyosin-dependent manner towards the cell centre. These unexpectedly dynamic changes in the morphology, molecular components and locations of cell–matrix adhesions contrast with the idea of classical focal contacts as stable cell attachments, and provide multiple mechanisms for cell interactions with the ECM.

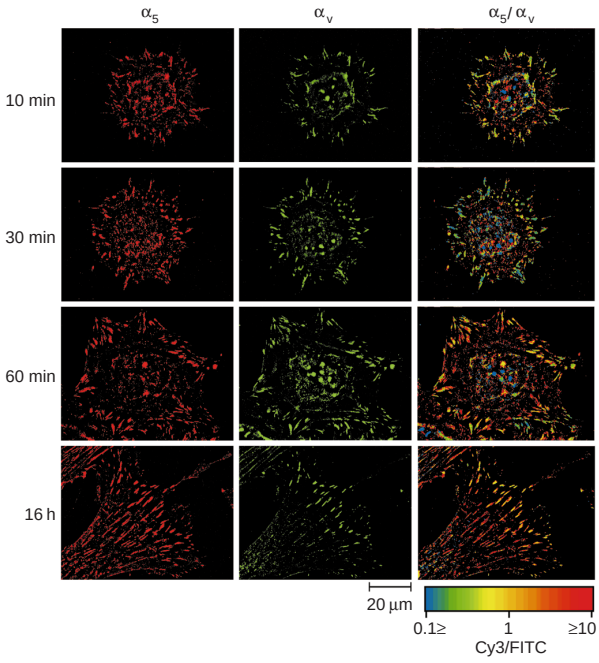

Figure 1 **Relative distributions of α_5 and α_v integrins in HFFs at different times after plating on fibronectin-coated coverslips.** HFFs were fixed and double-labelled for α_5 and α_v integrins. The columns, from left to right, show α_5 labelling with Cy3 (in red), α_v labelling with FITC (in green), and the quantitative, comparative, FRIC images (α_5/α_v), at the indicated time points. At early time points note the co-localization of α_v and α_5 integrins but the quantitative predominance (lower α_5/α_v ratio) of α_v, compared with the clear segregation of α_v and α_5 integrins in focal contacts and fibrillar adhesions after 16 h of incubation. The spectrum scale indicates the value of the ratio, as described in Methods.

Results

The molecular composition of early cell–matrix adhesions. To study the dynamic segregation of components of matrix adhe-

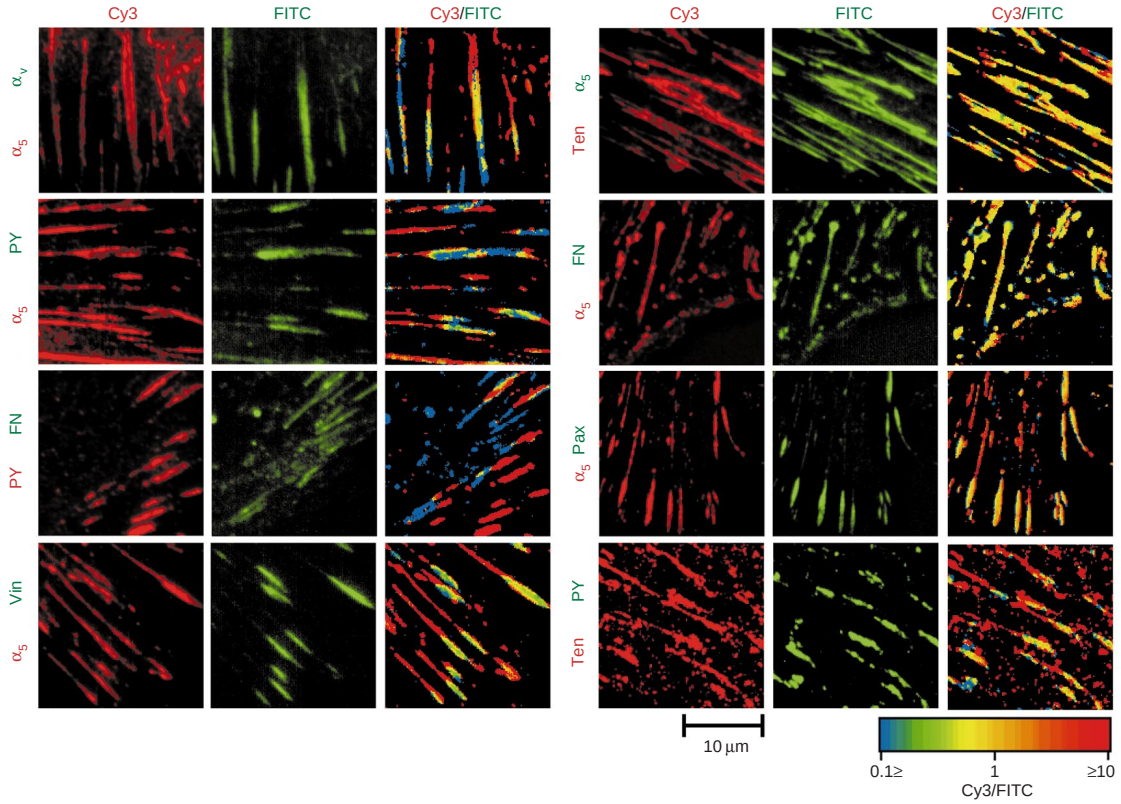

Figure 2 **Distributions of different components of focal contacts and fibrillar adhesions.** HFFs were fixed 16 h after plating, double-labelled for different pairs of plaque components using Cy3- and FITC-coupled antibodies, and subjected to FRIC analysis. The component names are coloured red if the antibody used to detect them was tagged with Cy3, and green if the antibody used for detection was tagged with FITC. Notice the segregation of focal-contact components (α_v integrin, paxillin, vinculin and phosphotyrosine) and fibrillar-adhesion components (α_5 integrin, tensin and fibronectin) into the respective adhesions, or into distinct zones in 'mosaic adhesions'. FN, fibronectin; Pax, paxillin; PY, phosphotyrosine; Ten, tensin; Vin, vinculin.

sion sites after plating human foreskin fibroblasts (HFFs) on fibronectin. Matrix adhesions immunolabelled for both α_5 and α_v integrins formed rapidly after plating on fibronectin and increased in number and size (Fig. 1). For the first hour after plating, the two integrins remained largely co-localized, although the relative labelling intensities for α_5 and α_v, reflected by the fluorescence ratio imaging between two different components (FRIC) values, changed as a function of time after plating. Thus, the relative levels of integrin α_v in adhesion sites (compared with levels of α_5) increased between 10 and 30 min; by 60 min, the distributions of integrins α_5 and α_v had partially segregated and segregation was complete after several hours. By 16 h, these integrins had segregated into classical focal contacts, which were enriched in α_v integrin, and fibrillar adhesions, containing α_5 integrin (for example, compare the α_5/α_v FRIC values in Fig. 1). Various other components of ECM adhesions segregated over time into two distinct structures (Fig. 2; see also refs 10, 11). Focal contacts contained relatively high levels of α_v integrin, vinculin, paxillin and phosphotyrosine, and relatively low levels of tensin, whereas fibrillar adhesions were enriched in α_5 integrin, fibronectin and tensin. In addition, 'mosaic adhesions' with subdomains exhibiting the molecular properties of both adhesions were apparent. These sites were polar, being enriched with fibrillar-adhesion components at their medial aspects and focal-contact components in their peripheral regions.

Dynamic reorganization of paxillin-containing focal contacts. To study the dynamic properties of focal contacts, we transfected HFFs with complementary DNAs encoding GFP–paxillin, and examined the organization of focal contacts by time-lapse fluorescence microscopy. We chose paxillin because it is particularly enriched in classical focal contacts, and is almost undetectable by immunofluorescence microscopy in fibrillar adhesions. Indeed, when expressed in HFFs, the GFP–paxillin fusion protein was associated only with focal contacts (Fig. 3). We used only trace levels of GFP–paxillin relative to levels of the endogenous protein, and the intensities and patterns of paxillin immunolabelling in transfected cells were indistinguishable from those of untransfected neighbouring cells. Analysis of time-lapse movies of GFP–paxillin (see Supplementary Information, movie 1) and temporal fluorescence ratio imaging (FRIT) analysis (Fig. 3) revealed several specific types of change. First, the assembly and growth of focal contacts involves the formation of new adhesions, generally at the cell periphery (red patches produced by FRIT indicate *de novo* adhesions; Fig. 3A, B, a). The growth of focal contacts is characterized either by their polar extension, always towards the cell centre (Fig. 3A, B, c), or by a uniform increase in total focal-contact area. Second, focal contacts, particularly small contacts (with areas of $<3\ \mu m^2$) and peripheral focal contacts, translocate frequently in HFFs. Translocation is highly directional, proceeding centripetally from the cell periphery towards the centre, and is always aligned along the long axis of the focal contacts (Fig. 3A, B, d). This translocation occurs at $19\pm11\ \mu m\,h^{-1}$ and is not a smooth, continuous process, but rather consists of a phase of centripetal extension followed by apparent 'contraction' of the trailing end of the focal contacts, reminiscent of inchworm movement (Fig. 3). This result is in agreement with previous observations[12–15]. Third, the fading of focal contacts, that is, a uniform decrease in GFP–paxillin intensity (Fig. 3A, B, b; blue), is a common process, con-

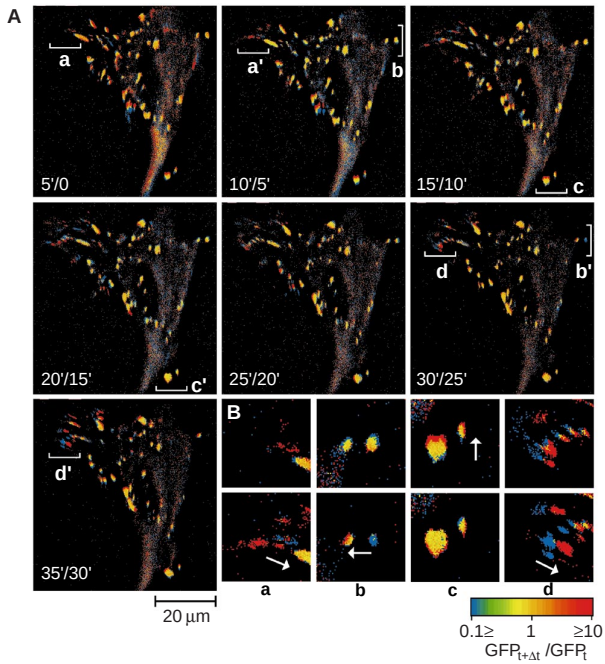

Figure 3 **Temporal changes in the pattern of GFP–paxillin labelling in transfected HFFs, as determined by FRIT. A**, Cells were analysed by time-lapse recording at 1-min intervals, starting 24 h after transfection with GFP–paxillin. The dynamic behaviour of GFP–paxillin is shown here by the FRIT patterns obtained from images taken at 5-min intervals (see Supplementary Information, movie 1). For example, the top left panel compares the image taken at 5 min with that taken at time 0. **B**, To exemplify different specific types of dynamic behaviour, four regions of the FRIT images (marked **a**–**d**) were magnified threefold from the earlier and later time windows shown in **A**. The magnified images are shown in **B** (upper row, earlier time points; lower row, later time points). The locations of the sampled regions in **A** are indicated by the brackets labelled **a**–**d** for the earlier time points and **a′**–**d′** for the later timepoints. The arrows point toward the cell centre.

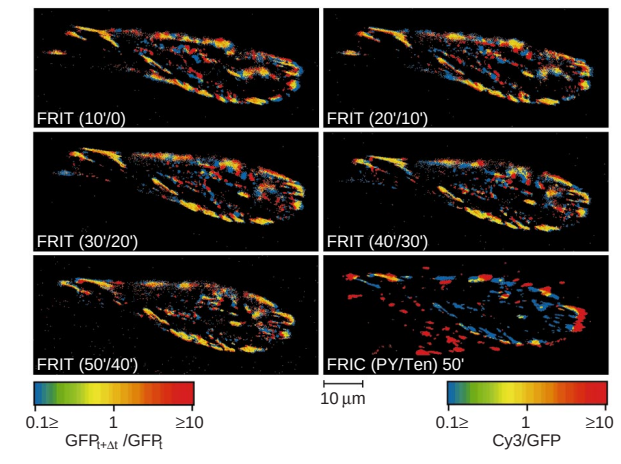

Figure 4 **Temporal (FRIT) analysis of GFP–tensin-transfected HFFs and FRIC analysis of phosphotyrosine residues and tensin.** Cells were analysed by time-lapse fluorescence recording starting 24 h after transfection with GFP–tensin. The dynamic behaviour of GFP–tensin is demonstrated by FRIT analysis of pairs of images taken at 10-min intervals. (See Supplementary Information, movie 2.) At the end of the live recording (50 min), the cells were fixed and immunolabelled for phosphotyrosine (PY). The FRIC image in the lower right panel shows the variability in the phosphotyrosine/tensin ratio between and within adhesion sites. Ten, tensin.

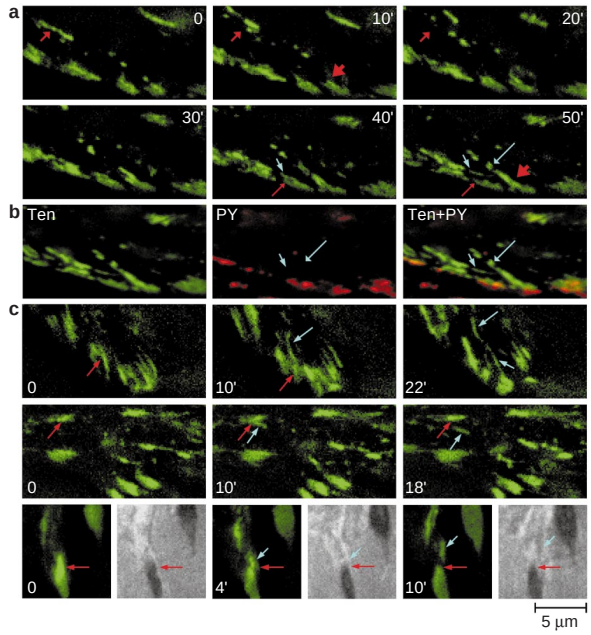

Figure 5 **High-magnification demonstration of the dynamics of tensin-containing structures and their phosphotyrosine content.** To highlight the dynamics of fibrillar adhesions, red arrows are located at fixed points (usually pointing to focal contacts) and blue arrows follow the movement of the fibrillar adhesions. **a**, A small region of the cell shown in Fig. 4 was magnified, and the localization of GFP–tensin at 10-min intervals is shown. **b**, The localization of GFP–tensin (Ten; in green) and immunolabelled-phosphotyrosine (PY; in red) in the same cell, fixed at 50 min. The blue arrows at 50 min in **a** and in the PY and Ten+PY images in **b** indicate the absence of phosphotyrosine from tensin-containing structures that emerged from focal contacts. **c**, Further examples, from other cells, of the emergence of tensin fibrils from focal contacts. In the bottom row, pairs of GFP–tensin (left-hand panel of each set of two panels) and interference-reflection-microscopy (right-hand panel of each set of two) images indicate that tensin fibrils emerging from focal contacts are often not associated with interference-reflection-dark structures.

sistent with the results of interference-reflection-microscopy studies[16,17].

The generation and translocation of fibrillar adhesions. To compare the dynamic properties of fibrillar adhesions and focal contacts, we transfected HFFs with cDNA encoding a GFP–tensin fusion protein. In agreement with the results of immunolocalization studies (Fig. 2; see also refs 10, 11), GFP-tagged tensin was mainly associated with fibrillar adhesions; weak labelling of classical focal contacts was also seen (Fig. 4).

Time-lapse microscopy of GFP–tensin revealed short, tensin-containing fibrils emerging from the medial ends of classical focal contacts and then translocating towards the cell centre (see Supplementary Information, movie 2). The short tensin-rich structures often merged with each other to form characteristic elongated fibrillar adhesions. These newly formed structures contained little or no paxillin, vinculin, focal-adhesion kinase (FAK) (ref. 10 and data not shown) or phosphotyrosine (Figs 4, Fig. 5b) and were initially often not associated with interference-reflection-dark structures (Fig. 5c).

FRIT images (Fig. 4) of GFP–tensin revealed two general patterns of reorganization. In one pattern, tensin-containing focal contacts moved slowly, primarily along cell margins (yellow structures in FRIT analysis, Fig. 4). In the second pattern, highly dynamic tensin-rich fibrillar adhesions were seen in more central locations (Fig. 4); note the predominance of red structures (which represent the presence of GFP–tensin in new locations) and blue colouring (which represents GFP–tensin-labelled structures that

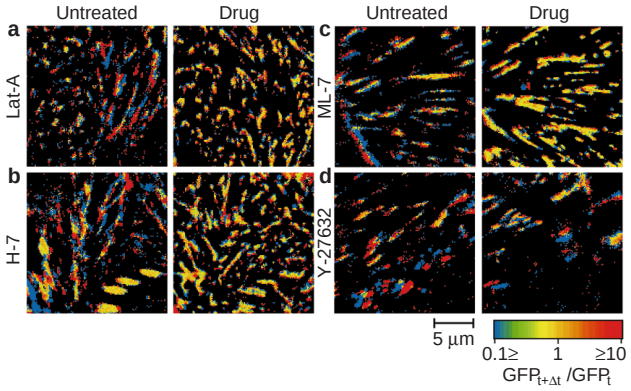

Figure 6 **Effects of cytoskeletal drugs on the mobility of tensin-containing structures.** HFFs were transfected with cDNA encoding GFP–tensin and analysed by time-lapse fluorescence recording before and during treatment with **a**, latrunculin-A (lat-A), **b**, H-7, **c**, ML-7, or **d**, the Rho-kinase inhibitor Y-27632. Temporal changes were analysed by FRIT from images taken at 10-min intervals before and during the drug treatments. Note the dynamic nature of fibrillar adhesions before treatment (indicated by the abundance of red or blue structures; stationary focal contacts appear yellow). **a–c**, Latrunculin-A, H-7 and ML-7 block the movement of these adhesions, as indicated by the abundance of yellow patterns. **d**, Y-27632 has only a limited effect, at this time point, on the structure and translocation of fibrillar adhesions, but had a dramatic effect on the stability of focal contacts. See also Supplementary Information, movies 3–6.

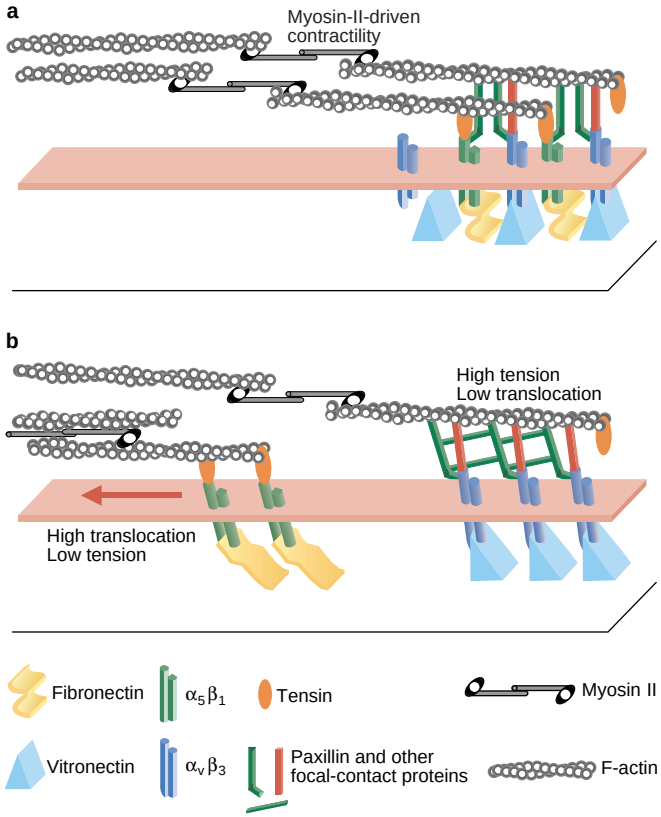

Figure 7 **Model for the involvement of actomyosin-driven forces in the formation and segregation of fibrillar adhesions and focal contacts. a**, Before segregation of focal contacts and fibrillar adhesions, the adhesion site contains $\alpha_v\beta_3$ integrin bound mainly to the ECM protein vitronectin, together with $\alpha_5\beta_1$ integrin bound mainly to fibronectin. Both integrins are associated through different plaque proteins with actin filaments (F-actin), and are subject to actomyosin-driven contraction forces. **b**, As vitronectin provides a rigid substrate, $\alpha_v\beta_3$ integrin does not move as a result of these contractile forces, and high tension develops, resulting in the recruitment of proteins typical of focal contacts, such as paxillin and vinculin, and in an increase in levels of phosphorylated tyrosine residues. In contrast, $\alpha_5\beta_1$, which is bound to the moveable fibronectin matrix, is moved by actomyosin pulling. Because tension is low, tension-dependent recruitment of paxillin, vinculin and phosphotyrosine residues does not occur. The association of fibrillar-adhesion components, such as tensin, is tension-independent; such components remain associated and translocate with $\alpha_5\beta_1$ integrin and the associated fibronectin.

had disappeared) in this region.

As shown in Fig. 5a, GFP–tensin fibrils also translocated laterally (small red arrows at time points 0, 10 min and 20 min, or at time points 40 min and 50 min). Staining of GFP–tensin-transfected cells for phosphotyrosine revealed nearly mutually exclusive tensin and phosphotyrosine patterns (Fig. 4, bottom right; Fig. 5b). More examples of tensin fibrils emerging from focal contacts are shown in Fig. 5c and in Supplementary Information, movies 3 and 4 (before drug addition; see below).

The actin cytoskeleton and fibrillar adhesion dynamics. To test the hypothesis that the formation and movement of fibrillar adhesions are actomyosin-driven processes, we perturbed the actin cytoskeleton using a variety of drugs. Latrunculin-A (2 µM), which destroys actin microfilaments by sequestering actin monomers, caused a rapid arrest in the formation and translocation of fibrillar adhesions. The results of the FRIT analysis shown in Fig. 6a reveal the immobilization of GFP–tensin after treatment with latrunculin-A, as demonstrated by the predominance of temporally overlapping structures (coloured yellow in the FRIT image; see also Supplementary Information, movie 3). Moreover, inhibition of serine and threonine phosphorylation by 150 µM H-7 (Fig. 6b) or 100 µM ML-7 (Fig. 6c) (both block activity of the myosin-light-chain kinase) resulted in destruction of actin bundles and focal contacts. This treatment also rapidly inhibited the translocation of tensin-containing fibrillar adhesions, but had only minor effects on their structure (Fig. 6b, c; see also Supplementary Information, movies 4, 5). All three types of drug did not disrupt existing fibrillar adhesions. The observed effects were fully reversible after washing out latrunculin-A, H-7 or ML-7.

We also tested for an involvement of Rho kinase in tensin translocation, as Rho-driven activation of Rho kinase stimulates actomyosin contractility[18,19]. Treatment of GFP–tensin-transfected cells with the Rho-kinase inhibitor Y-27632 (ref. 20), even at 100–300 µM, had only a limited inhibitory effect on the stability or translocation of fibrillar adhesions (Fig. 6d). However, tensin was rapidly lost from the centre of focal contacts as a result of such treatment, and focal contacts were subsequently destroyed completely (see also Supplementary Information, movie 6).

Discussion

Here we searched for dynamic changes in cell–ECM adhesions in cultured human fibroblasts. We focused on the main classes of matrix adhesion — focal contacts and fibrillar adhesions — using dynamic microscopic analyses of GFP-tagged paxillin or tensin. Both classes of adhesion are associated with integrins and actin, but their subcellular localization and detailed molecular composition are markedly different: focal contacts contain relatively high levels of $\alpha_v\beta_3$ integrin, paxillin and vinculin, and only modest levels of $\alpha_5\beta_1$ and tensin; are usually located at the ends of actin stress fibres; and are highly tyrosine phosphorylated. In contrast, fibrillar adhesions contain only $\alpha_5\beta_1$ integrin and are characteristically enriched only in tensin, lacking the other plaque components studied and tyrosine phosphorylation. In addition, fibrillar adhesions are associated with fibronectin fibrils close to the cell centre, whereas focal

contacts often bind fibronectin-free ECM sites at the cell periphery[10,21].

These two types of matrix adhesion appear to differ not only in their shape and molecular composition, but also in their functions[11,22,23] (R. Pankov, personal communication). Focal contacts are characteristically found about 10–20 nm from the ECM substrate and mediate tight cell–substrate adhesion. In contrast, fibrillar adhesions (also termed ECM contacts) are found ≤100 nm from the substrate, and $\alpha_5\beta_1$ integrin mediates binding to fibronectin fibrils, adhesion, slowing of cell migration and assembly of a fibronectin matrix. Because only the focal contacts are highly tyrosine phosphorylated and contain FAK[10], they are probably also the major site of integrin signalling. Thus, it is important to understand how these two distinct forms of cell–matrix adhesion are generated.

Our results show that fibrillar adhesions assemble at one pole of focal contacts and are actively transported from these sites. This conclusion is based on direct visualization of tensin-rich fibrils emerging centripetally from focal contacts and then translocating towards the cell centre. This dynamic process depends on the presence of an intact microfilament system and active myosin II, as actin disruption or inhibitors of myosin-light-chain kinase block both the formation of fibrillar adhesions and their translocation. The initial stage of fibrillar-adhesion formation occurs at the margin of focal contacts orientated towards the cell centre. This finding explains our previous static immunofluorescence results which showed that, in addition to focal contacts and fibrillar adhesions, there exist 'mosaic adhesions' characterized by a polar segregation of subdomains enriched either in tensin, α_5 integrin and fibronectin or in vinculin, paxillin, phosphotyrosine residues and α_v integrin (Fig. 2; see also ref. 10). These mosaic adhesions appear to represent early stages of fibrillar-adhesion formation, before the fibrillar adhesions segregate completely from focal contacts.

On the basis of our present results and previous data, we propose the following model for the assembly and segregation of focal contacts and fibrillar adhesions (Fig. 7). First, upon interaction with the ECM, integrins ($\alpha_5\beta_1$, $\alpha_v\beta_3$ and potentially other integrins) bind to the matrix, cluster, and interact across the membrane with specific plaque proteins and actin filaments[24,25] (Fig. 7a). These structures may be analogous to the 'focal complexes' induced by Rac[26,27]. Second, actomyosin-driven forces act on these new complexes. As focal-contact-associated actin filaments are orientated with their barbed (more slowly growing) ends towards the membrane[28], tension is applied primarily from the membrane towards the cell centre.

Third, the outcome of these forces depends on the physical properties of the associated matrix. Thus, interaction with a deformable or pliable matrix such as substrate-adsorbed fibronectin results in translocation of the ECM component together with specific integrins and tensin (Fig. 7b). This process appears to be responsible for fibronectin fibrillogenesis (R. Pankov, personal communication). In contrast, interactions with a rigid, non-deformable matrix (such as glass-associated vitronectin) lead to immobilization of adhesion complexes, high tension at the cytoskeleton–membrane interface, and assembly of focal contacts[13,14,29,30] (Fig. 7b). It is likely that local, tension-driven activation of tyrosine phosphorylation produces new docking sites for a variety of anchor and signalling molecules that become associated with the developing focal contacts. When fibronectin translocation is prevented by covalently immobilizing it to the substrate, large focal contacts form without fibrillar adhesions, and the components of focal contacts and fibrillar adhesions remain intermixed[11]. We propose that transformation or generation of fibrillar adhesions at focal contacts is governed by a mechanical switch, namely matrix deformability or pliability. This mechanical regulator would provide cells with the capacity to respond to environmental cues, such as a rigid substrate, by switching to an adhesion mode that provides firm anchorage.

Fourth, although large, paxillin-rich focal contacts are generally stationary, small focal contacts can translocate, in agreement with the results of previous studies that were based on tandem scanning confocal microscopy[14], fluorescence microscopy of microinjected talin, vinculin or α-actinin[12,13], or the expression of GFP–β_1-integrin fusion proteins[15]. The movement of these small focal contacts involves polar extension at one end of the focal contact followed by contraction of the other end in an inchworm-like process. This movement of non-immobilized small focal contacts also appears to depend on contractile actomyosin.

A specific cell type may emphasize only one adhesion mechanism. For example, fibronectin fibrils and fibrillar adhesions are the most common structures for NIL8 cells[31], whereas chicken lens and other cells show focal contacts at sites from which fibronectin is actively removed[21]. In cells that can switch on the formation of fibrillar adhesions from focal contacts, the initial presence of $\alpha_5\beta_1$ integrin in focal contacts immediately after plating of cells on fibronectin and the replacement of $\alpha_5\beta_1$ by $\alpha_v\beta_3$ can be explained by the ligand specificity of these integrins, with $\alpha_v\beta_3$ binding to vitronectin and $\alpha_5\beta_1$ binding to fibronectin, after the fibronectin is cleared away into fibrils from under focal contacts[21,32,33].

In summary, the unexpected dynamics and diverse range of changes in the morphology, molecular constituents and locations of cell–matrix adhesions identified here provide cells with a rich, varying palette of adhesion structures beyond the classical stationary focal contacts. This diversity and flexibility is consistent with the multitude of parts known to be played by cell–ECM adhesions. The apparent function of matrix deformability as a mechanical switch that regulates the transition from focal contacts to fibrillar adhesions may be only one of many mechanisms for integrating these important processes. □

Methods

GFP fusion proteins.

Full-length human paxillin cDNA (provided by K. Nakata, S. Miyamoto and K. Matsumoto) or full-length chicken tensin cDNA[34] were ligated into the GFP expression vector pGZ21 as described[35].

Cells and immunofluorescence labelling.

Primary HFFs were cultured, treated and labelled for immunofluorescence in serum-containing medium as described[10,11]. Drugs included H-7 or ML-7 (Sigma), latrunculin-A (provided by I. Spector), and Y-27632 (Yoshitomi Pharmaceuticals Industries, Saitama, Japan).

Electroporation.

Subconfluent HFFs were suspended in electroporation buffer (20 mM HEPES, 137 mM NaCl, 5 mM KCl, 0.7 mM Na_2HPO_4 and 6 mM dextrose, pH 7.05) and either GFP–paxillin or GFP–tensin vector (30 μg), and electroporated using a GENE PULSER II (Bio-Rad)[36]. Following electroporation, cells were collected by centrifugation, resuspended with DMEM, and plated (see below).

Digital microscopy and time-lapse recording.

The methods for image acquisition have been described previously[10]. For dynamic microscopic analyses, glass coverslips were glued with hot wax to the bottom of 35-mm tissue-culture plates, and then coated with 25 μg ml^{-1} fibronectin. HFFs were transfected with GFP–paxillin or GFP–tensin cDNA, plated on the tissue-culture plates, and examined microscopically. For time-lapse recording, cells were maintained in DMEM with 10% fetal calf serum buffered with 10 mM HEPES, pH 7.0 at 37 °C. Images were acquired every 1 or 2 min using a filter set for GFP.

Image processing.

Fluorescence ratio imaging between two different components (FRIC) using double-labelled cells was done as described[10]. In short, Cy3 and fluorescein isothiocyanate (FITC) or GFP images were subjected to high-pass filtration to remove background labelling and to avoid the generation of 'noisy' images resulting from the presence of low-intensity pixels in the numerator or denominator. Ratio values were calculated pixel by pixel and displayed using a spectrum scale[10]. The same principle was applied for temporal fluorescence ratio imaging (FRIT) to compare images of GFP fluorescence acquired at two different time points. In FRIT, the numerator and the denominator correspond to the later and earlier images, respectively. Thus, a red colour indicates a new structure and a blue colour indicates a structure that has disappeared.

RECEIVED 21 OCTOBER 1999; REVISED 18 JANUARY 2000; ACCEPTED 1 FEBRUARY 2000; PUBLISHED 22 FEBRUARY 2000.

1. Howe, A., Aplin, A. E., Alahari, S. K. & Juliano, R. L. Integrin signaling and cell growth control. *Curr. Opin. Cell Biol.* **10**, 220–231 (1998).
2. Gumbiner, B. M. Cell adhesion: the molecular basis of tissue architecture and morphogenesis. *Cell* **84**, 345–357 (1996).
3. Yamada, K. M. & Geiger, B. Molecular interactions in cell adhesion complexes. *Curr. Opin. Cell Biol.* **9**, 76–85 (1997).
4. Clark, E. A. & Brugge, J. S. Integrins and signal transduction pathways: the road taken. *Science* **268**,

233–239 (1995).
5. Schoenwaelder, S. M. & Burridge, K. Bidirectional signaling between the cytoskeleton and integrins. *Curr. Opin. Cell Biol.* **11,** 274–286 (1999).
6. Jockusch, B. M. *et al.* The molecular architecture of focal adhesions. *Annu. Rev. Cell. Dev. Biol.* **11,** 379–416 (1995).
7. Geiger, B., Yehuda-Levenberg, S. & Bershadsky, A. D. Molecular interactions in the submembrane plaque of cell-cell and cell-matrix adhesions. *Acta Anat.* **154,** 46–62 (1995).
8. Schwartz, M. A., Schaller, M. D. & Ginsberg, M. H. Integrins: emerging paradigms of signal transduction. *Annu. Rev. Cell. Dev. Biol.* **11,** 549–599 (1995).
9. Hynes, R. O. Integrins: versatility, modulation, and signaling in cell adhesion. *Cell* **69,** 11–25 (1992).
10. Zamir, E. *et al.* Molecular diversity of cell-matrix adhesions. *J. Cell Sci.* **112,** 1655–1669 (1999).
11. Katz, B. Z. *et al.* Physical state of the extraxellular matrix regulates the structure and molecular composition of cell-matrix adhesions. *Mol. Biol. Cell* (in the press).
12. Kreis, T. E., Avnur, Z., Schlessinger, J. & Geiger, B. in *Molecular Biology of the Cytoskeleton* (eds Borisy, G., Cleveland, D. & Murphy, D.) 45–57 (Cold Spring Harb. Symp., Cold Spring Harbor, 1985).
13. Hock, R. S., Sanger, J. M. & Sanger, J. W. Talin dynamics in living microinjected nonmuscle cells. *Cell Motil. Cytoskeleton* **14,** 271–287 (1989).
14. Davies, P. F., Robotewskyj, A. & Griem, M. L. Endothelial cell adhesion in real time. Measurements in vitro by tandem scanning confocal image analysis. *J. Clin. Invest.* **91,** 2640–2652 (1993).
15. Smilenov, L. B., Mikhailov, A., Pelham, R. J., Marcantonio, E. E. & Gundersen, G. G. Focal adhesion motility revealed in stationary fibroblasts. *Science* **286,** 1172–1174 (1999).
16. Izzard, C. S. & Lochner, L. R. Formation of cell-to-substrate contacts during fibroblast motility: an interference-reflexion study. *J. Cell Sci.* **42,** 81–116 (1980).
17. Izzard, C. S. & Lochner, L. R. Cell-to-substrate contacts in living fibroblasts: an interference reflexion study with an evaluation of the technique. *J. Cell Sci.* **21,** 129–159 (1976).
18. Kimura, K. *et al.* Regulation of myosin phosphatase by Rho and Rho-associated kinase (Rho-kinase). *Science* **273,** 245–248 (1996).
19. Amano, M. *et al.* Phosphorylation and activation of myosin by Rho-associated kinase (Rho-kinase). *J. Biol. Chem.* **271,** 20246–20249 (1996).
20. Uehata, M. *et al.* Calcium sensitization of smooth muscle mediated by a Rho-associated protein kinase in hypertension. *Nature* **389,** 990–994 (1997).
21. Avnur, Z. & Geiger, B. The removal of extracellular fibronectin from areas of cell-substrate contact. *Cell* **25,** 121–132 (1981).
22. Chen, W. T. & Singer, S. J. Immunoelectron microscopic studies of the sites of cell-substratum and cell-cell contacts in cultured fibroblasts. *J. Cell Biol.* **95,** 205–222 (1982).
23. Akiyama, S. K., Yamada, S. S., Chen, W. T. & Yamada, K. M. Analysis of fibronectin receptor function with monoclonal antibodies: roles in cell adhesion, migration, matrix assembly, and cytoskeletal organization. *J. Cell Biol.* **109,** 863–875 (1989).
24. Miyamoto, S. *et al.* Integrin function: molecular hierarchies of cytoskeletal and signaling molecules. *J. Cell Biol.* **131,** 791–805 (1995).
25. Plopper, G. & Ingber, D. E. Rapid induction and isolation of focal adhesion complexes. *Biochem. Biophys. Res. Commun.* **193,** 571–578 (1993).
26. Nobes, C. D. & Hall, A. Rho, rac, and cdc 42 GTPases regulate the assembly of multimolecular focal complexes associated with actin stress fibers, lamellipodia, and filopodia. *Cell* **81,** 53–62 (1995).
27. Rottner, K., Hall, A. & Small, J. V. Interplay between Rac and Rho in the control of substrate contact dynamics. *Curr. Biol.* **9,** 640–648 (1999).
28. Begg, D. A., Rodewald, R. & Rebhun, L. I. The visualization of actin filament polarity in thin sections. Evidence for the uniform polarity of membrane-associated filaments. *J. Cell Biol.* **79,** 846–852 (1978).
29. Bershadsky, A., Chausovsky, A., Becker, E., Lyubimova, A. & Geiger, B. Involvement of microtubules in the control of adhesion-dependent signal transduction. *Curr. Biol.* **6,** 1279–1289 (1996).
30. Chrzanowska-Wodnicka, M. & Burridge, K. Rho-stimulated contractility drives the formation of stress fibers and focal adhesions. *J. Cell Biol.* **133,** 1403–1415 (1996).
31. Hynes, R. O. & Destree, A. T. Relationships between fibronectin (LETS protein) and actin. *Cell* **15,** 875–886 (1978).
32. Fath, K. R., Edgell, C. J. & Burridge, K. The distribution of distinct integrins in focal contacts is determined by the substratum composition. *J. Cell Sci.* **92,** 67–75 (1989).
33. Singer, II *et al.* Cell surface distribution of fibronectin and vitronectin receptors depends on substrate composition and extracellular matrix accumulation. *J. Cell Biol.* **106,** 2171–2182 (1988).
34. Chuang, J. Z., Lin, D. C. & Lin, S. Molecular cloning, expression, and mapping of the high affinity actin-capping domain of chicken cardiac tensin. *J. Cell Biol.* **128,** 1095–1109 (1995).
35. Kioka, N. *et al.* Vinexin: a novel vinculin-binding protein with multiple SH3 domains enhances actin cytoskeletal organization. *J. Cell Biol.* **144,** 59–69 (1999).
36. LaFlamme, S. E., Thomas, L. A., Yamada, S. S. & Yamada, K. M. Single subunit chimeric integrins as mimics and inhibitors of endogenous integrin functions in receptor localization, cell spreading and migration, and matrix assembly. *J. Cell Biol.* **126,** 1287–1298 (1994).

ACKNOWLEDGEMENTS
This study was supported by the Israel Science Foundation, the Yad Abraham Center for Cancer Diagnosis and Therapy, and the Minerva Foundation. B.G. holds the Erwin Neter Chair in Cell and Tumor Biology. Z.K. holds the Israel Pollak Chair of Biophysics. We thank D. Rivelin and G. Tzur for advice regarding time-lapse recording and digital microscopy.
Correspondence and requests for materials should be addressed to B.G.
Supplementary information is available on *Nature Cell Biology*'s World-Wide Web site (www.nature.com/ncb).

Supplementary Information is available for this article. The movies that correspond to the captions below can be found by selecting "suppl info" on the Nature Cell Biology Web page.

Movie Legends

Movie 1 Time-lapse recording of an HFF cell expressing GFP–paxillin. Images were recorded at 1-min intervals starting 24 h after transfection. Time is indicated by the time bar. GFP–paxillin is localized in focal contacts, and their dynamic behaviour, namely assembly and growth, translocation and fading, can be appreciated. These changes are highlighted by FRIT analysis in Fig. 3 of the paper. Bar indicates 10 μm.

Movie 2 Time-lapse recording of an HFF cell (and twofold-magnified inserts of the same and two other cells) expressing GFP–tensin. Images were recorded at 2-min intervals starting 24 h after transfection. Time is indicated by the time bar. GFP–tensin is localized in both focal contacts and fibrillar adhesions, and thus reveals the dynamic relationships between the two. Tensin-containing fibrils emerge from the medial ends of focal contacts and then translocate toward the cell centre. This dynamic behaviour is highlighted in Fig. 5 and by FRIT analysis in Fig. 4 of the paper. Scale bar represents 10 μm.

Movie 3 Time-lapse recording of an HFF cell expressing GFP–tensin, before, during and after incubation with 2 μM latrunculin-A. Images were recorded at 2-min intervals starting 24 h after transfection. Time is indicated by the time bar, and the timing of drug addition and removal is marked by arrows. Scale bar represents 10 μm.

Movie 4 Time-lapse recording of an HFF cell expressing GFP–tensin, before, during and after incubation with 150 μM H-7. Images were recorded at 2-min intervals starting 24 h after transfection. Time is indicated by the time bar, and the timing of drug addition and removal is marked by arrows. Scale bar represents 10 μm.

Movie 5 Time-lapse recording of an HFF cell expressing GFP–tensin, before, during and after incubation with 100 μM ML-7. Images were recorded at 2-min intervals starting 24 h after transfection. Time is indicated by the time bar, and the timing of drug addition and removal is marked by arrows. Scale bar represents 10 μm.

Movie 6 Time-lapse recording of two HFF cells expressing GFP–tensin, before, during and after incubation with 100 μM (left cell) or 300 μM (right cell) Y-27632. Images were recorded at 2-min intervals starting 24 h after transfection. Time is indicated by the time bar, and the timing of drug addition and removal is marked by arrows. Scale bar represents 10 μm.